Steel Grips

JOURNAL OF STEEL AND RELATED MATERIALS

www.steel-grips.com

Application

GRIPS Intermedia GmbH
ISSN 1866-8453

online

2011

T. Aseer Brabin, Thankian Christopher, and B. Nageswara Rao:

Assessing the failure of cylindrical pressure vessels due to longitudinal weld misalignment

Failure assessment was made on cylindrical pressure vessels containing longitudinal weld misalignment performing finite element analysis (FEA) utilizing the Ansys software package. A 20° section of the cylindrical shell wall was modeled utilizing the plane strain element (plane 182) with the longitudinal weld in the centre of section. The weld misalignment was introduced by shifting the position of the cylindrical section on one side of the weld relative to the other section. Failure pressure estimates from FEA based on the global plastic deformation are found to be in good agreement with existing test results on vessels made of Afnor 15CDV6 steel and maraging steels.

In the design of pressure vessels, certain regions frequently exist where continuity of the structure cannot be satisfied by membrane forces alone. Such regions are known as *discontinuity areas.* Determination of discontinuity stresses is an important problem, i.e. the design of pressure vessels. Discontinuity stress can arise from three basic sources:

⇒ geometric discontinuity: abrupt change in radius of curvature and/or thickness of the shell;

⇒ material discontinuity: abrupt change in mechanical properties;

⇒ load discontinuity: abrupt change in load intensity of static loading - *line load*.

In practical situations these causes may, of course, appear singly or in any combinations. The linear elastic analysis of thin shells of revolution is well founded and prediction of stresses in such structures can be made with relatively high accuracy. For simple shell geometries, solutions to the discontinuity problem were obtained in closed form [1...9].

Johns and Orange [1] presented general linear equations in terms of edge-influence coefficients for the bending moment and shear force at a shell junction, including the effect of an axi-symmetric misalignment in a thin-walled pressure vessel. Johns et al. [3] examined experimentally the effect of misalignment on the stress distributions in pressurized shells. They found good agreement between the experiment and the elastic solutions of Johns and Orange [1] for the cases of circular cylindrical pressure vessels with a continuous inner surface or a continuous outer surface at a change in thickness at a circumferential joint. Wittrick [5] provided a nonlinear solution for the discontinuity stresses at an axi-symmetric junction between very thin shells of revolution, including the effect of misalignment at the joint. Johns [6] described a simple method for determining misaligned stresses in a pressure vessel, with results given for a circumferential joint in circular cylinders. The analysis is applicable only to shells of constant thickness, and stresses are found only at junction.

The prediction of failure pressure that a cylindrical pressure vessel can withstand is an important consideration in the design of pressure vessels. These require the study of two models of failure viz. yielding and fracture [10]. Failure due to yielding occurs when some functional of stress or strain is exceeded and fracture occurs when an existing crack extends. Various methods are being used to estimate the maximum failure pressure [11...15]. S. Rao et al. [14] discussed the effects of weld misalignment on the load bearing capacity of the motor case, failure pressure estimates and their validation through burst pressure estimation of motor case. They presented a simple expression for failure pressure estimates of rocket motor cases having weld misalignment. The failure pressure estimates are found to be in good agreement with the burst pressure test results of maraging steel motor cases. For more complex geometries, finite element analysis (FEA) utilizing the commercial software packages (viz., Ansys, Nisa, Marc, etc.) will be more appropriate.

To understand the combined stress theories of failure and their use in design, FEA was carried out for assessing the failure of unflawed steel cylindrical pressure vessels from the measured properties of uni-axial tensile specimens [16]. An axi-symmetric four-node quadrilateral finite element (element type: 2 D plane 42) available in Ansys software package is utilized to model the cylindrical pressure vessel. Axial displacement is suppressed at both ends of the cylindrical shell to have no axial growth under internal pressure. Ansys has the provision for checking the global plastic deformation (GPD). It indicates the pressure levels to cause complete plastic flow through the cylinder wall (i.e. bursting pressure). Failure pressure estimations from FEA considering GPD will be useful to asses the life of complex structures made of ductile materials.

In the fabrication of large rocket motor cases, weld joints are inevitable and controlled welding is very difficult to achieve, leading to misalignments at the weld joints. These misalignments cause stress concentration near the weld joints. Min et al. [17] performed parametric studies to determine the influence of weld offsets and the variation of weld widths in longitudinally welded cylindrical structures with equal wall thickness on both sides of the joint. In general, the stress field varies continuously along the meridian of a pressure vessel dome. Also, flight loads and hydrostatic pressures produce variations in stress along the meridian, as well as circumferentially, in most propellant tanks. Knowing the resultant misalignment stresses in any stress field is, therefore, desirable. It should be noted that an axi-symmetric four-node quadrilateral element can be used for analyzing the pressure vessels having a misalignment in a circumferential joint [18].

Three-dimensional (3D) finite element modelling is required for analyzing pressure vessels, or rocket motor cases having longitudinal weld misalignments. It is noted that the cylindrical portion of the rocket motor casing, in general, will be stressed maximum under internal pressure and, hence, governs the design. During burst testing of rocket motor cases [11; 14], it is observed that the growth of the cylindrical shell in axial direction is negligibly small compared to its length and the material becomes incompressible at the initiation of instability, which indicates excessive deformation in circumferential direction. The four-node quadrilateral, isoparametric plane strain element available (plane 182) in Ansys is more appropriate to model the longitudinal weld misalignment in a cylindrical vessel. Motivated by the work of above mentioned authors, FEA was carried out utilizing Ansys software package to access the failure of maraging steel rocket motor cases having longitudinal weld misalignment. Failure pressure estimates from FEA (based on GPD) are found to be in good agreement with test results [14] of maraging steel rocket motor cases.

Empirical relations for bursting pressure

Faupel's empirical relation [19] is modified for the burst pressure estimates of cylindrical vessels and demonstrated its validity through comparison of existing test results and those obtained from the Svensson's bursting pressure formula [20] for power-law hardening materials. A modification of Faupel's empirical relation for the burst pressure (p_b) is [15; 16]:

$$p_b = \frac{2}{\sqrt{3}}\sigma_{ys}\left\{1+0.65\left(1-\frac{\sigma_{ys}}{\sigma_{ult}}\right)\right\} ln\left(\frac{R_o}{R_i}\right) \quad (1)$$

where R_o and R_i are the outer and inner radii of the cylindrical vessel; σ_{ys} is the yield strength of the material and σ_{ult} is the ultimate tensile strength of the material.

Worswick and Pick [21] derived the collapse pressure (p_c) of an open end cylindrical pipes in the presence of long-seam misalignment as:

$$p_c = \frac{t}{R_i}\left\{\sqrt{1+\left(\frac{\delta}{t}\right)^2}-\frac{\delta}{t}\right\}\sigma_{ys} \quad (2)$$

where t is the thickness and δ is the measure of misalignment. For δ = 0, the collapse pressure (p_c) in equation (2) represents the case where the hoop stress σ_{hoop} $\left(=\frac{PR_i}{t}\right)$ under internal pressure is equal to the yield strength (σ_{ys}) of the material. In the case of closed-end thin-walled cylindrical shells, a biaxial gain factor has to be applied to the collapse pressure. For high strength maraging steels, yield strength σ_{ys} is close to the ultimate tensile strength σ_{ult}. Equation (1) clearly indicates the biaxial gain factor of $\frac{2}{\sqrt{3}}$ (≈ 1.154). The hoop stress concentration factor due to weld offset is given by [7; 17]: $K_1 = 1+3\frac{\delta}{t}$. The effective stress magnification factor K_{eff} associated with the long-seam misalignment in the cylindrical vessel is [7]:

$$K_{eff} = \sqrt{1+6\frac{\delta}{t}+12\left(1-\nu+\nu^2\right)\left(\frac{\delta}{t}\right)^2}. \quad (3)$$

Poisson's effect in equation (3) can be neglected by replacing the Poisson's ratio (ν) as zero for relatively short misalignments whose length is less than $5\sqrt{R_i t}$. If the vessel is loaded beyond the proportional limit of the material, a possibility of reduction in the elastic effective stress magnification factor K_{eff} will exist. The plastic stress magnification factor K_p is [14]:

$$K_p = 1+\left(K_{eff}-1\right)\frac{E_s}{E}, \quad (4)$$

where E is the Young's modulus and E_s is the secant modulus. If the vessel is loaded within the proportional limit of the material, $E_s = E$ and $K_p = K_{eff}$. For thin-walled cylindrical vessels made of power-law hardened materials, the secant modulus E_s^* at the initiation of instability is [14]:

$$E_s^* = \frac{\sqrt{3}}{n}\left(\frac{e}{\sqrt{3}}\right)^n \sigma_{ult},$$

here, n is the strain hardening exponent of the material.

Failure pressure $p_{b\delta}$ of a cylindrical vessel having long-seam misalignment is:

$$p_{b\delta} = \frac{p_b}{K_P}. \quad (5)$$

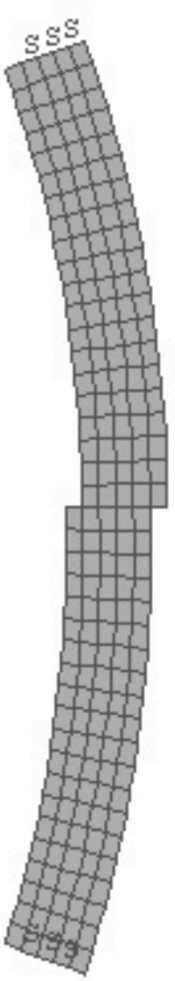

Fig. 1: Plane strain finite element model of the cylindrical vessel with longitudinal weld misalignment

Results of finite element analysis

Finite element analysis (FEA) was carried out on cylindrical pressure vessels having misalignment in the longitudinal weld. For failure pressure estimations, the four-node quadrilateral and isoparametric plane strain element (plane 182) of Ansys which has both geometric and material non-linear capabilities is considered in the present study. A 20° section of the cylindrical shell was modelled with the longitudinal weld in the centre of the section as shown in **fig. 1**. The ends of the sections were constrained (symmetric boundary conditions) to displace in the radial direction only, while a

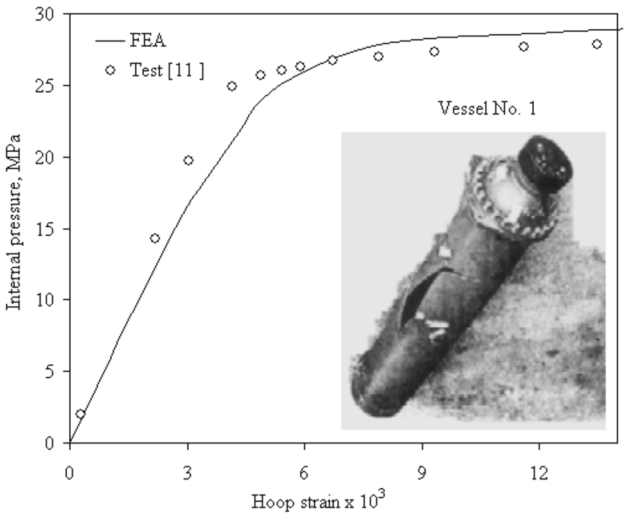

Fig. 2: Comparison of finite element analysis results with measured hoop strains for the applied internal pressure at the outer surface of the cylindrical vessel made of Afnor 15CDV6 steel (vessel No. 1)

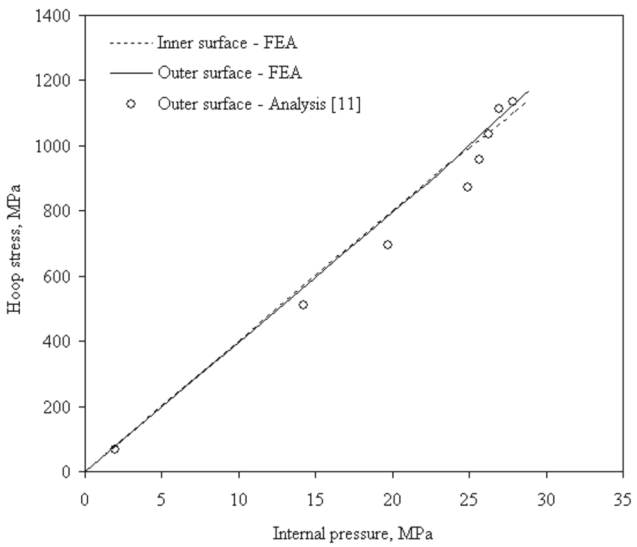

Fig. 3: Variation of hoop stress with the applied internal pressure in a cylindrical vessel made of Afnor 15CDV6 steel (vessel No. 1)

uniform pressure was applied along the inner surface of the section. The weld misalignment was introduced by shifting the position of the cylindrical sections on one side of the weld relative to the other section.

A constitutive relationship that gives stress as an explicit function of strain is useful in the finite element analysis. The relationship is [11; 16]:

$$\sigma = E\,\varepsilon\left\{1+\left(\frac{\varepsilon}{\varepsilon_o}\right)^{n_o}\right\}^{\frac{-1}{n_o}} \qquad (6)$$

where $\varepsilon_o = \frac{\sigma_{ult}}{E}$, σ_{ult} is the tensile strength of the material and n_o is the parameter defining the shape of the non-linear stress-strain relationship. The single valued expression (6) represents essentially the inverse of Ramberg-Osgood´s equation. Material properties of the cylindrical pressure vessels made of Afnor 15CDV6 steel and maraging steels are presented in **table 1**.

Table 1: Material properties of pressure vessels made of Afnor 15CDV6 steel and maraging steels (Poisson's ratio ν = 0.3)

Vessel No.	Young's modulus *E*	yield strength σ_{ys}	ultimate tensile strength σ_{ult}	material constants in eq. (6)	
	GPa	MPa	MPa	ε_o	n_o
		Afnor 15CDV6 steel [11]			
1	204.0	915	1060	0.0050	3.98
		maraging steels [14]			
2 to 6	186.3	2128	2155	0.0116	12.12
7	186.3	1646	1667	0.0089	10.36
8	186.3	1651	1710	0.0092	7.31

The number of elements and nodes for the cylindrical pressure vessels analyzed in the absence of longitudinal weld misalignment (vessel number 1 to 6) are 216 and 247 respectively. The number of elements and nodes for the cylindrical pressure vessels analyzed with longitudinal weld misalignment (vessel number 7) is 1040 and 1166 respectively, whereas for vessel number 8 these are 2600 and

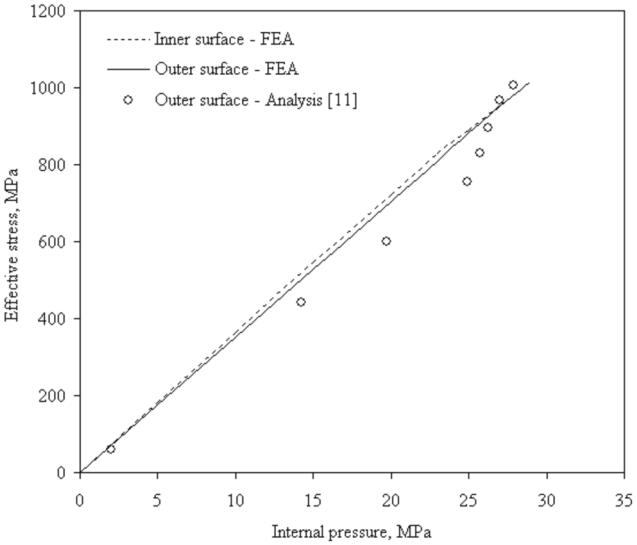

Fig. 4: Variation of effective stress with the ap plied internal pressure in a cylindrical vessel made of Afnor 15CDV6 steel (vessel No. 1)

Table 2: Burst pressure estimations for the 90-mm flow formed maraging steel motor cases

Vessel No.	thickness mm	failure pressure, MPa test [13]	eq.(1)	relative error, %	FEA	relative error, %
2	1.630	86.6	88.1	-1.8	88.5	-2.2
3	1.756	94.5	94.8	-0.4	95.0	-0.5
4	1.793	94.0	96.8	-3.0	97.0	-3.2
5	1.763	94.0	95.2	-1.3	95.5	-1.6
6	1.735	92.3	93.7	-1.5	94.0	-1.8

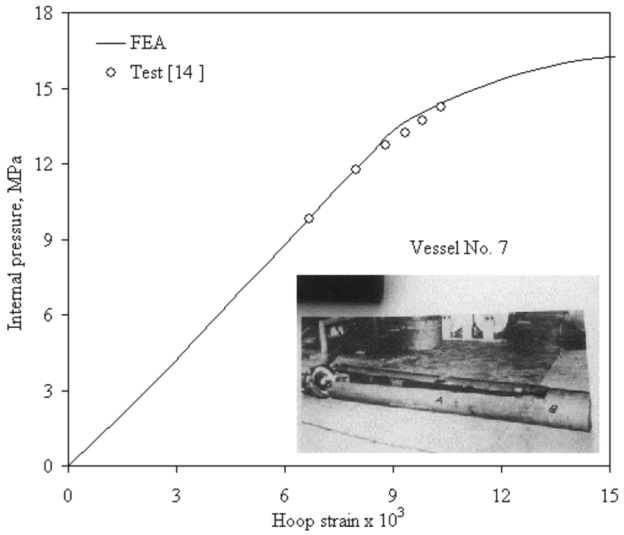

Fig. 5: Comparison of finite element analysis results with measured hoop strains for the applied internal pressure at the longitudinal weld misalignment on the outer surface of the cylindrical vessel made of M250 grade maraging steel (vessel No. 7)

2772, respectively. Convergence study was performed by analyzing the models with higher mesh density.

Fig. 2 shows a good comparison of finite element analysis results with measured hoop strains [11] for the applied internal pressure of Afnor 15CDV6 steel vessel. The failed 2.6 mm thick cylindrical vessel having an outer diameter D_o of 212 mm is also shown in fig. 2. Variation of the hoop stress and the effective stress in the cylindrical shell portion of the steel vessel with the applied internal pressure is shown in **figs. 3** and **4**. The bi-axial gain factor (i.e., the ratio of hoop stress to the effective stress at failure pressure) is: 1171.1/1015.8 = 1.1529 MPa. The failure pressure estimated from the finite element analysis is 29 MPa, which

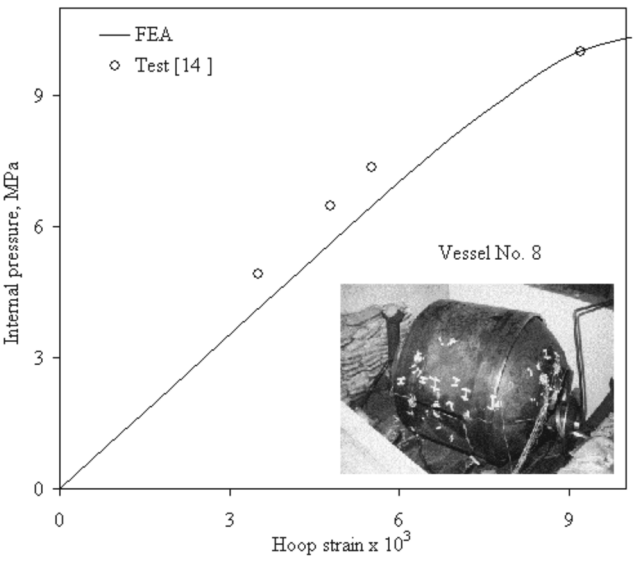

Fig. 6: Comparison of finite element analysis results with measured hoop strains for the applied internal pressure at the longitudinal weld misalignment on the outer surface of the cylindrical vessel made of M250 grade maraging steel (vessel No. 8)

is found to be in good agreement with the actual burst pressure value of 28.86 MPa [11]. **Table 2** gives the burst pressure estimations of 90 mm diameter flow formed maraging steel motor cases (vessel number 2 to 6). The failure pressure estimates are found to be within ±3.2 % of the test results [13].

S. Rao et al. [14] presented the test data on two rocket motor cases (vessel numbers 7 and 8) made of M250 grade maraging steel. Vessel number 7 is a 1.5 mm thick cylindrical vessel having 303 mm outer diameter and 0.3 mm longitudinal weld misalignment (20 % of shell wall thickness). The strain hardening exponent n of the material is 0.032.

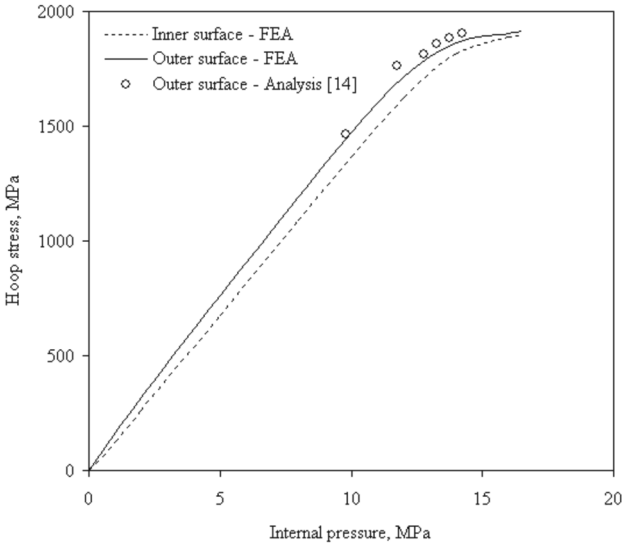

Fig. 7: Variation of hoop stress with the applied internal pressure in a cylindrical vessel made of M250 grade maraging steel (vessel No. 7)

The axial and hoop strains measured close to the long-seam misalignment of the motor case at 14.22 MPa pressure level are 2478 and 10322 μm, respectively. The effective stress σ_{eff} at this pressure level is worked out to be 1648 MPa, which is slightly higher than the yield strength of the material. Applying the biaxial gain factor of 1.154 to the collapse pressure p_c of 13.5 MPa from equation (2), it is possible to estimate the allowable pressure as 15.58 MPa, whereas equation (5) gives $p_{b\delta}$ as 14.7 MPa. The actual burst pressure of the motor case is 15.2 MPa. Vessel number 8 is a 5.6 mm thick cylindrical vessel having 2011 mm outer diameter and 0.28 mm longitudinal weld misalignment (5 % of shell wall thickness). The strain hardening exponent n of the material is 0.04842. The axial and hoop strains measured close to the long-seam misalignment of the motor case at 10 MPa pressure level are 1517 and 9209 μm, respectively. The effective stress σ_{eff} at that pressure level is worked out to be 1570 MPa. Applying the biaxial gain factor of 1.154 to the collapse pressure p_c of 8.79 MPa from equation (2), it is possible to estimate the allowable pressure as 10.14 MPa, whereas equation (5) gives $p_{b\delta}$ as 10.18 MPa. The actual burst pressure of the motor case is 10.25 MPa.

Figs. 5 and **6** show the comparison of finite element analysis results with measured hoop strains for the applied internal pressure at the longitudinal misalignment on the outer surface of the cylindrical vessels (vessel numbers 7 and 8) made of M250 grade maraging steel. The finite element analysis gives the failure pressure for vessel number 7 and 8 as 16.5 MPa and 10.6 MPa, resp., whereas the actual burst pressures reported in ref. [14] are 15.2 MPa and 10.25 MPa, respectively. The finite element analysis results were found to be in reasonably good agreement with the actual burst pressure values reported. **Figs. 7** to **10** show the variation of hoop and effective stress of the vessels at maximum stress location with respect to the internal pressure. Finite element elasto-plastic analysis provides reasonably good failure pressure estimates of pressure vessels with and without misalignment.

Conclusions

Finite element analysis has been carried out using the Ansys software package to estimate the failure pressure of cylindrical vessels having longitudinal weld misalignment. Failure pressure estimates from FEA based on global plastic deformation were found to be in good agreement with existing test results. Closed form solutions are available for the determination of failure pressure of regular shaped cylindrical pressure vessels. However, finite element analysis is essential to simulate elasto-plastic behaviour and, hence, to determine failure pressure of cylindrical pressure vessels with misalignment at joints.

References

[1] R.H. Johns and T.W. Orange: Theoretical elastic stress distribution arising from discontinuities and edge loads in several shell type structures, NASA TR R-103, 1961.

[2] W.C. Morgan and P.T. Bizon: Experimental investigation of stress distributions near abrupt change in wall thickness in thin walled pressurized cylinders, NASA TN D-1200, 1962.

[3] R.H. Johns, W.C. Morgan and D.A. Spera: AIAA Journ. 1 (1963), p. 4557/57.

[4] W.C. Morgan and P.T. Bizon. Experimental evaluation of theoretical elastic stress distribution for cylinder-to-hemisphere and cone-to-sphere junctions in pressurized shell structures, NASA TN D-1565; 1963.

[5] W.H. Wittrick: Intern. Journ. Eng. Sci. 2 (1964), p. 179/88.

[6] R.H. Johns: AIAA Journ. 2 (1964), p. 1827/28.

[7] R.H. Johns: Theoretical elastic mismatch stresses, NASA TN D-3254, 1966.

[8] W.C. Morgan and P.T. Bizon: Comparison of experimental and theoretical stresses at a mismatch in a circumferential joint in a cylindrical pressure vessel, NASA TN D-3608, 1966.

[9] P.T. Bizon: Elastic stresses at a mismatched circumferential joint in a pressurized cylinder including thickness changes and meridional load coupling, NASA TN D-3609, 1966.

[10] B. N. Rao: Enging. Fract. Mechan. 43 (1992), p. 455/59.

[11] A.P. Beena, M.K. Sundaresan and B. N. Rao: Intern. Journ. Pressure Vessels & Piping 62 (1995), p. 313/20.

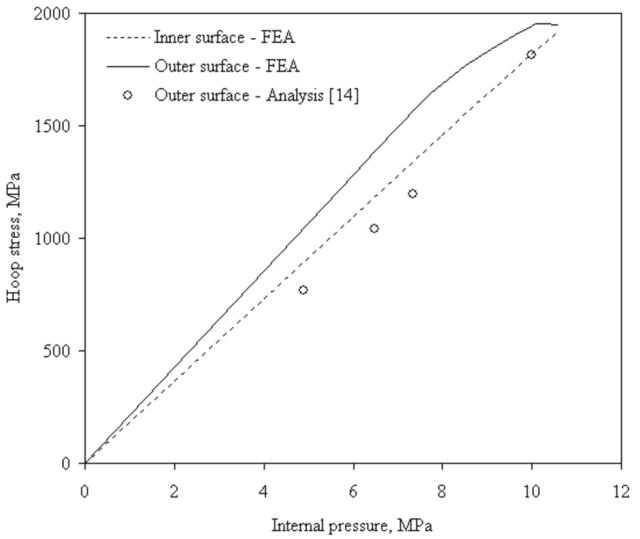

Fig. 9: Variation of hoop stress with the applied internal pressure in a cylindrical vessel made of M250 grade maraging steel (vessel No. 8)

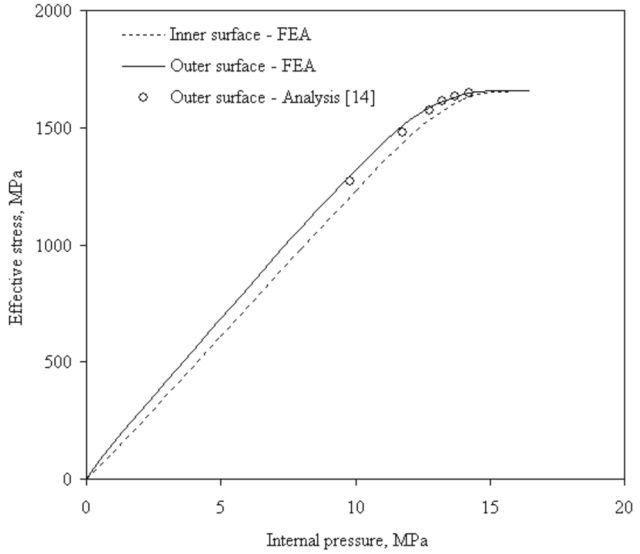

Fig. 8: Variation of effective stress with the applied internal pressure in a cylindrical vessel made of M250 grade maraging steel (vessel No. 7)

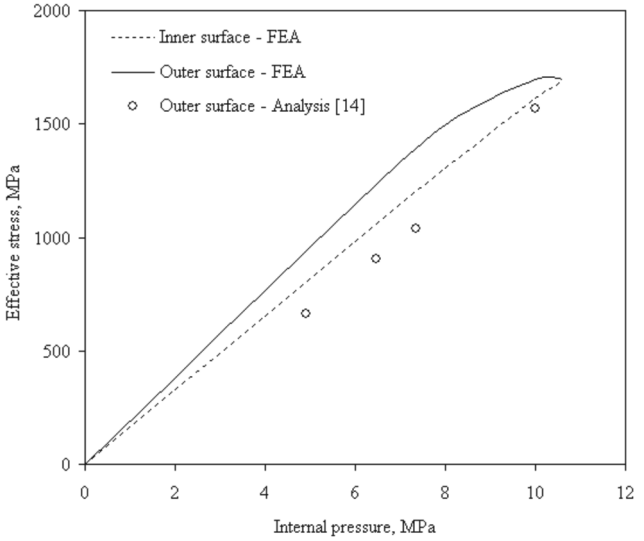

Fig. 10: Variation of effective stress with the applied internal pressure in a cylindrical vessel made of M250 grade maraging steel (vessel No. 8)

[12] T. Christopher, B.S.V. Rama Sarma, P.K.G. Potti, B. N. Rao and K. Sankaranarayanasamy: Intern. Journ. Pressure Vessels & Piping 79 (2002), p. 53/66.
[13] J. Margetson: Burst pressure prediction of rocket motors, 14th AIAA/SAE Joint Propulsion conf., Las Vegas, NV, USA, Paper No.78-1567, 1978.
[14] A. S. Rao, G. V. Rao, B. N. Rao: Engineer. Fail. Anal. 12 (2005), p. 325/36.
[15] T. A. Brabin, T. Christopher and B. N. Rao: Intern. Journ. Pressure Vessels & Piping 88 (2011), p. 119/22.
[16] T. A. Brabin, T. Christopher, B. N. Rao: Mater. Struct. 5 (2009), p. 29/42.
[17] J.B. Min, K.L. Spanyer and R.M. Brunair: Parametric study in weld mismatch of longitudinally welded SSME HPFTP inlet" NASA-TM-103534, 1991.
[18] T. A. Brabin, T. Christopher and B. N. Rao: Intern. Journ. Pressure Vessels & Piping 87 (2010), p. 197/201.
[19] J.H. Faupel: Trans. ASME Journ. Appl. Mechan. 23 (1956), p. 1031/64.
[20] N.L. Svensson: Trans. ASME Journ. Appl. Mechan. 25 (1958), p. 89/96.
[21] W.J. Worswick and R.J. Pick: Journ. Pipeline 5 (1986), p. 221/29.

Dr. T. Aseer Brabin
Principal
Universal College of Engineering & Technology
Vallioor

Dr. Thankian Christopher
Head & Professor of Mechanical Engineering
Government College of Engineering
Tirunelveli

B. Nageswara Rao
Structural Analysis and Testing Group
Vikram Sarabhai Space Centre
Trivandrum

India